

Photoinduced dynamics in a photosensitive side chain polymeric liquid crystal by quasielastic and inelastic neutron scattering

L. Cristofolini,¹ M. P. Fontana,¹ M. Laus,² and B. Frick³¹*Dipartimento di Fisica and INFN, Università di Parma, Parco Area delle Scienze 7/A, I-43100 Parma, Italy*²*Università del Piemonte Orientale, Alessandria, Italy*³*ILL, Avenue des Martyrs, 38042 Grenoble, France*

(Received 8 June 2001; published 27 November 2001)

We report the first study by inelastic (INS) and quasielastic neutron scattering of photoinduced changes in the reorientational and vibrational dynamics of a liquid crystalline side chain polymer. We use the *cis-trans* photoisomerization transition to take the system out of equilibrium and determine the quasielastic (QE) and inelastic scattering laws on two distinct time windows, corresponding to the time-of-flight (IN6) and backscattering (IN16) spectrometers at Institut Laue Langevin (ILL) (Grenoble). Our investigation was focused on the dynamics of the coupling between the mesogenic side chains and the polymeric main chain, which is connected to the extensive optical writing and memory effects that have been demonstrated in this complex material. We report data on the QE broadening and Debye-Waller factors, as a function of temperature across the glass transition ($T_g = 293$ K). We also studied the dynamical coupling of side and main chains. We report photoinduced changes on the static structure factor, on the purely elastic scattering fraction, on the low frequency vibrational dynamics (around the boson peak region). In particular, we find that on the space-time scales accessible to the INS techniques there is a time structure in the coupling, and that over longer times and distances the two dynamics are decoupled.

DOI: 10.1103/PhysRevE.64.061803

PACS number(s): 61.12.-q, 61.30.Vx, 64.70.Pf, 63.50.+x

I. INTRODUCTION

Side chain polymeric liquid crystals have been extensively studied for their strong potential as functional materials with the mechanical properties of plastics [1]. Of particular interest are azobenzene-based systems, in which the photoinduced *cis-trans* isomerization of the azobenzene moiety in the side chain has been used to generate several interesting optical effects with possible application to high density optical memories [2]. The liquid crystalline properties of the azobenzene moiety are preserved in the polymeric macromolecule by the device of attaching the mesogenic azobenzene to the main polymeric chain via a so-called flexible spacer, i.e., a polymethylene chain, with an optimal number of units of the order of 6. Such number determines the equilibrium between two conflicting requirements: the necessity of decoupling the side chain from the main chain, so that the liquid crystalline phase may be realized and the necessity of a sufficiently strong interaction of the side chain with the main chain, so that extensive and stable memory effects are obtained.

A particularly interesting member of the family of azobenzene-based photosensitive polymers is a polyacrylate, whose structure is reported in Fig. 1, for which strong and extensive optical effects have been demonstrated [3,4]. This material was also studied from a more fundamental point of view, being a prototype fragile glass former ($T_g = 293$ K) [5,6]. For example, the possibility of taking the polymeric glass out of equilibrium via optical excitation of the *cis-trans* isomerization has provided an interesting way of studying molecular relaxation in the neighborhood of the glass transition [7]. In all these studies, the role of the coupling between the main chain and the side chains is deemed to be essential;

however, little is known about such coupling and how it affects the molecular dynamics, both from the point of view of the glass transition and of optical memory effects.

In this paper, we present a study of molecular dynamics and relaxation following photoperturbation via excitation of the *cis-trans-cis* isomerization of the azobenzene side chain. The study was performed by quasielastic and inelastic neutron scattering with different time windows, following the photoinduced changes in the dynamics of either side or main chain on several time scales. In particular using time-of-flight spectroscopy, we covered the fast side chain motions (~ 10 ps); using backscattering and spin-echo spectroscopy, we are sensitive to slow motions up to the tens of nanoseconds scale. The main purpose of such measurements was to determine the eventual time structure of the coupling between main and side chains. We find, indeed, evidence for decoupling, as on the fast time scale we clearly find photoinduced changes in the dynamics, whereas no noticeable effect was detected on the slow time scale where the main chain is expected to contribute both directly (main chain dynamics) and indirectly (e.g., through the side chain methylenes close to the rigid units of the side chain).

II. EXPERIMENT

The specific polymer we studied was the poly([4-pentyloxy-3'-methyl-4'(6-acryloxyoxyloxy)]azo-benzene)

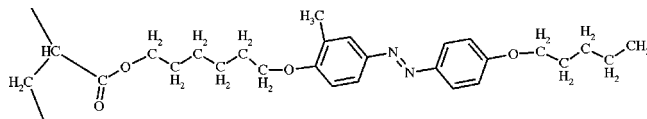


FIG. 1. Sketch of one repeat unit of the polymer PA4 poly([4-pentyloxy-3'-methyl-4'(6-acryloxyoxyloxy)]azo-benzene).

(PA4, shown in Fig. 1); we note that the PA4 monomeric unit counts only three protons in the main chain and 33 protons in the side chain, therefore, its incoherent cross section is largely dominated by the side chain contribution. The material was synthesized according to procedures reported elsewhere [8] and had molecular weight $M_w = 19\,000$, $M_n = 12\,000$ (weight and number averaged, respectively). The samples for the inelastic neutron scattering (INS) experiments were prepared as thick films deposited by the cast solution method on thin, copper free aluminum disks. In order to study photoinduced effects, the thickness of the sample could not exceed about $80\ \mu\text{m}$, due to the requirement of having a reasonably homogeneous optically modified sample. This in turn, placed rather stringent conditions on the signal-to-noise ratio (S/N) obtainable in our spectra, which was far from optimal. Optical excitation was accomplished using a high pressure 450 W xenon lamp, which illuminated the sample directly in the spectrometer hutch during the measurement through a quartz window added in the thermal screen of the suitably modified cryofurnace. Filters and polarizers were employed to cut the irradiation spectrum above the wavelength $\lambda = 500\ \text{nm}$, thus reducing the photoinduced *cis*-to-*trans* back relaxation and also excluding thermal heating of the sample (final power density on sample $\approx 50\ \text{mW/cm}^2$). Unavoidably the illumination equipment restricted the accessible Q range for the backscattering experiments. Spectra were taken before and during illumination, at selected temperatures in the range between 100 K and 373 K. We note that to our knowledge these are the first measurements of photoinduced dynamical changes as probed by neutron scattering.

As stated, in this work we studied the sample dynamics on several time scales. In particular, we used IN6, IN11, and IN16 spectrometers at ILL. For IN6, neutron wavelength was $5.4\ \text{\AA}^{-1}$, the available exchanged momentum range was $0.2\text{--}2.7\ \text{\AA}^{-1}$. The elastic resolution full width at half maximum (FWHM) was $0.10\ \text{meV}$. These parameters correspond to a space-time window of the experiment of up to 40 ps and from 0.2 to 3 nm. The slower time scales were probed with the backscattering spectrometer IN16 and the spin-echo spectrometer IN11. For the former, the available energy window was $\pm 15\ \mu\text{eV}$ and the elastic resolution FWHM $= 0.9\ \mu\text{eV}$ (approximately 4 ns). The slowest time scale was also probed directly with IN11, which allowed the intermediate scattering law $S(Q, t)$ to be followed for times up to 10 ns. Although one would expect in principle the spin-echo spectrometer IN11 to be able to follow $S(Q, t)$ up to longer times, this was precluded in the present case because some of the compensating Helmholtz coils had to be removed to make room for the cryostat, the Xe lamp and the associated optics. Therefore, the IN11 data only marginally extend those from IN16 and as such are discussed very briefly.

Data from IN6 and IN16 were corrected for detector efficiency, with a standard vanadium calibration and for the empty can contribution; data were summed over several detectors in order to improve the S/N ratio (at loss of resolution in the Q space); given the tiny amount of sample (limited by the constraint of achieving homogeneous UV illumination), no self-absorption (slab) correction was needed. The inelastic

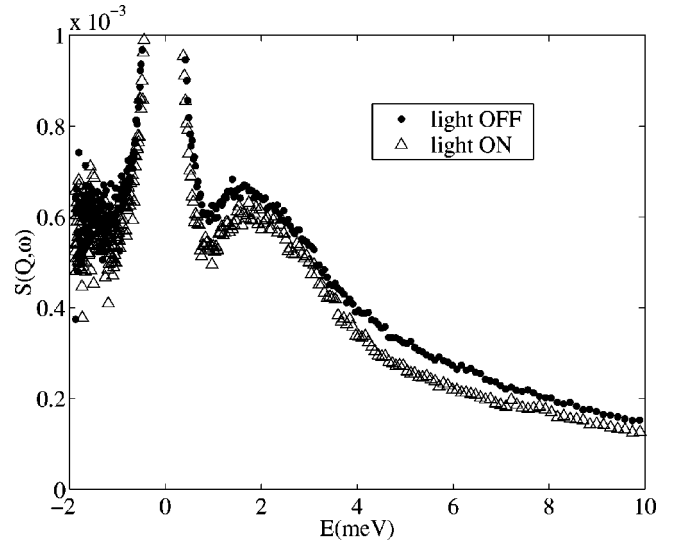


FIG. 2. Scattering law $S(Q, \omega)$ measured on PA4 at $T = 100\ \text{K}$ on IN6, before (filled circles) and under UV illumination (open triangles, see text). Each curve is normalized to the elastic peak intensity.

part of the IN6 spectra was reduced to a vibrational density of states using the standard ILL suite of programs [9]: we applied corrections for detailed energy balance and multiphonon contributions.

III. RESULTS AND DISCUSSION

We shall begin by discussing the results obtained on the fast time scale of IN6. In Fig. 2, we show the measured scattering law $S(Q, \omega)$ of a PA4 film before and under unpolarized UV light illumination, summing data from all the IN6 detectors. Each curve is normalized to the elastic peak intensity. A small but noticeable reduction of the inelastic intensity can be observed when UV light is switched on; we also note that such difference is not just a scale factor as it is energy dependent.

In Fig. 3, we present the neutron-weighted vibrational density of states $g(E)$, obtained at 100 K, where all the slow diffusional motion can be assumed to be frozen. In the figure, we show the effects of optical pumping and the corresponding difference spectrum. We note small but clear differences in the region of the excess modes in the vibrational density of states (VDOS) that originate the so-called “boson peak” [10] and a compensating change (so that the overall area under the $g(E)$ curve is kept constant) at higher energies; in particular the $g(E)$ intensity in the excess modes region is largely reduced upon UV illumination. Such effects decrease and vanish at the higher temperatures investigated. The region of the boson peak is related to acousticlike, more or less propagating (according to the different schools of thought [10]) collective excitations. In the present case this implies mainly the motions of the main chain, although, we cannot exclude a possible contribution from low frequency “accordion modes” in the side chain. However, in general such modes have higher frequency (e.g., in 4,4'-di-*n*-pentyloxyazoxybenzen (C5) the accordion mode is

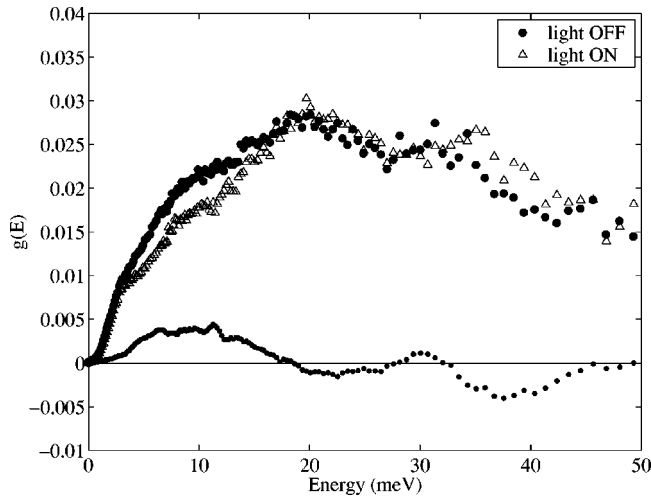


FIG. 3. Neutron-weighted vibrational density of states $g(E)$ for PA4 measured at $T=100$ K on IN6, without UV light (filled circles, see text for details) and with UV light (open triangles), also shown is the difference between the two.

found at 318 cm^{-1} [11], and in *N*-(*P*-ethoxybenzilidene)-*p*-*n*-butibaniline (EBBA) it is found at 280 cm^{-1} [12]). Thus, the present data indicate that the main chains are influenced by the light-induced reorientations of the side chains. The fact that UV illumination, and, hence, *trans*-to-*cis* isomerization, causes a large reduction in the intensity of the boson peak can be related to the fact that a large *cis* fraction implies a more fluid and, hence, homogeneous system. In particular, birefringence under polarizing microscope has shown that photoisomerized PA4 (by means of UV irradiation) is much softer and compliant to optical pumping [13]. Furthermore by AFM scanning force microscopy [14], by null ellipsometry [7] and by synchrotron x-ray reflectivity [15], we were able to show that UV irradiation reduces surface roughness and increases main chain mobility, also promoting thin film dewetting from energetically unfavorable surfaces.

We turn now to the analysis of the quasielastic range, which should be sensitive to the reorientational motion of the side chains and fast conformational fluctuations both in the main and side chains. As anticipated, a counting of the hydrogens, however, indicates that most of the scattered intensity is due to the side chain hydrogens. The spectra were fit using one elastic contribution (δ function) and one single QE contribution (with Lorentzian shape), both convoluted with the experimental resolution function as determined from the vanadium standard. From the fit of the QE Lorentzian, we obtain the behavior of the FWHM with Q , which, within our substantial error limits, turns out to be independent of Q . This indicates the presence of a localized reorientational motion as the source of the QE broadening.

Given the less than ideal quality of our data, we did not think appropriate to interpret the data with quantitative fits to specific models typical of liquid crystalline systems [16]. Assuming for simplicity the isotropic rotational diffusion model, from the measured values of the FWHM, we obtain the reorientational relaxation time scale, which turns out to be about 35 ± 5 ps at 200 K. We found, within our error

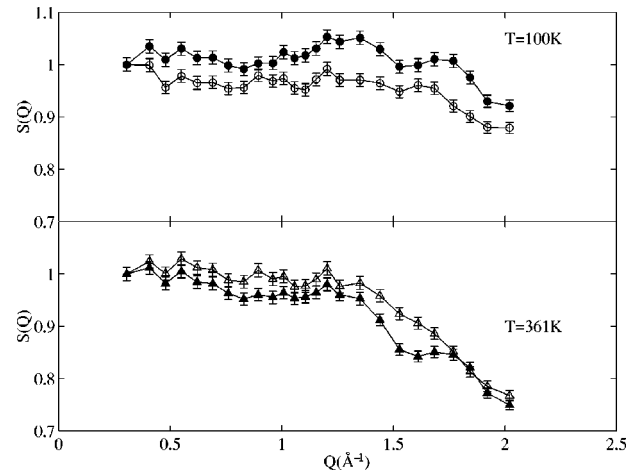


FIG. 4. The static structure factor [$S(Q)$ integrated over all the energy transfer range], for PA4 both with UV light off (filled symbols) and on (empty symbols). Top panel, data at $T=100$ K: note the small peaks at $Q=1.3 \text{ \AA}^{-1}$ and $Q=1.8 \text{ \AA}^{-1}$. Bottom panel: $T=361$ K, at high temperature the Debye Waller (DW) factor clearly reduces $S(Q)$ at high Q (note the change in the vertical scale) and also smears out the structural peaks.

limits no appreciable temperature dependence of the FWHM. We discuss this anomaly further on.

The optical pumping was found to accelerate the reorientational motion, yielding a corresponding relaxation time of about 23 ± 5 ps at the same temperature of 200 K. The optically induced change was found to decrease with increasing temperature. This is in agreement with our general finding that photoinduced changes in the dynamics are more pronounced at low temperatures, where all the thermally activated motions are more or less frozen.

The total scattered intensity $S(Q)$, obtained integrating over the whole energy transfer range accessible to IN6, is shown in Fig. 4 as a function of the momentum transfer Q , for both UV light off and on, at low temperature (top panel, $T=100$ K) and well above T_g (bottom panel, $T=361$ K). The measured $S(Q)$ contains both the incoherent and the coherent contributions to the total scattering law; the latter is the static structure factor, which can be considered a snapshot of the structure and is responsible for the small peaks observed in $S(Q)$ at low temperature (100 K), whereas at high temperature (361 K) the Q dependence is dominated by the Debye-Waller (DW) factor.

In Fig. 5, we report the logarithm (base 10) of the purely elastic fraction of the scattered intensity $S(Q, \omega=0)$ normalized to the static structure factor $S(Q)$, as a function of the momentum transfer squared Q^2 and for different sample temperatures. In such quantity the static structure factor is factorized out and the only residual Q dependence is due to the Debye-Waller factor: $\exp(-\frac{1}{3}Q^2\langle u^2 \rangle)$. The linear slopes in Fig. 5 give the DW mean square displacement $\langle u^2 \rangle$ at each temperature, which is shown as a function of the temperature in the inset of the same figure, together with the prediction of the harmonic approximation, (dotted line). The harmonic approximation is reasonably well obeyed up to T_g . At higher temperatures the observed additional increase of $\langle u^2 \rangle$ above

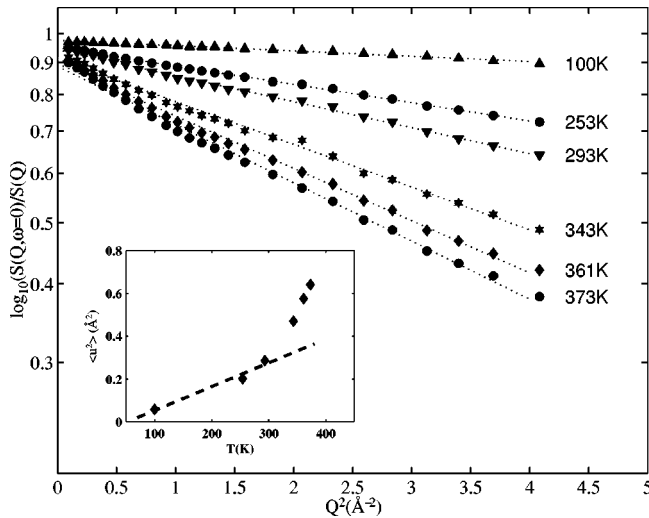


FIG. 5. Logarithm (base 10) of the elastic intensity $S(Q, \omega=0)$ normalized to the total intensity $S(Q)$, as a function of Q^2 , for different temperatures in PA4 as measured on IN6. The dashed lines correspond to the Debye-Waller fits at the different marked temperatures (see text). Inset: temperature dependence of the Debye-Waller mean square displacement $\langle u^2 \rangle$. The dashed line represents the harmonic approximation, well describing the experimental data up to $T_g = 293$ K.

the harmonic approximation may be ascribed to anharmonicity (as suggested also by the observed Q dependence of the elastic intensity) to the releasing of additional degrees of freedom (possibly related to the side chain) but we note that a similar upturn of $\langle u^2 \rangle$ above T_g is observed also in simpler main chain polymeric systems [17,18]. This is reasonable thinking that in our system the glass-to-melt transition is also controlled by the presence of the side chain, as is confirmed also by the general finding that in side chain polyacrylates T_g reduces (within certain limits, also given by the increasing entanglements) as the flexible spacer length and the end tail length are increased [19–21].

It is also of interest to study the photoinduced difference in the elastic signal $S(Q, \omega=0)$. This quantity contains information on the relative weight of elastic and inelastic contributions as well as, from its Q dependence, on the geometry of the reorientational diffusion, and its eventual space structure [17]. To understand its behavior, the coherent contribution to the total scattering law must be taken into account. In Fig. 6, we show the effect of optical pumping on $S(Q, \omega=0)$ at the temperatures of our experiment: the figure shows directly the light on–light off difference of the elastic signal. In the low temperature data, we note a clear structure in the Q dependence, which highlights two characteristic distances, corresponding to the minima. In particular, also looking at the Q dependence of the static structure factor $S(Q)$ shown in the top panel of Fig. 4, it appears evident that the minima that we observe in the 100 K curve of Fig. 6 that are located at $Q=0.5$ and 1.3 \AA^{-1} , (corresponding closely in real space to the characteristic size of the azobenzene in the *trans* and *cis* conformations, ~ 13 and $\sim 5 \text{ \AA}$, respectively), result from the disappearance of a corresponding peak in $S(Q)$ measured in the dark and to a depression of $S(Q)$ measured

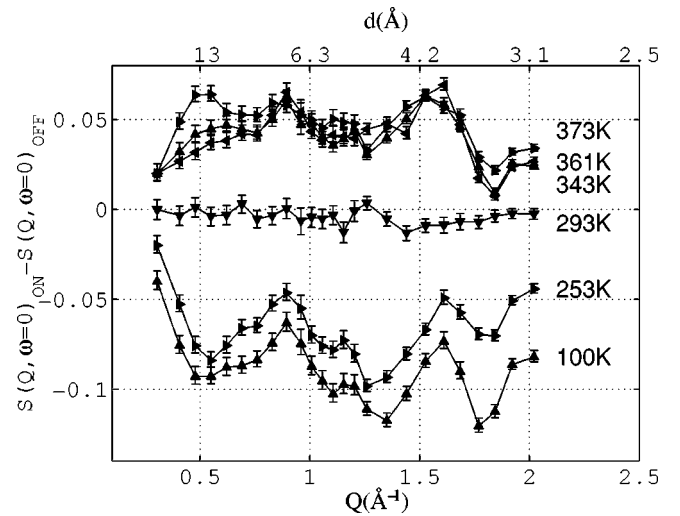


FIG. 6. Difference in the elastic signal $S(Q, \omega=0)$ as measured with UV light on minus the same quantity measured without UV light (see text for details), as a function of the exchanged momentum Q in PA4 at different temperatures.

with UV light on, respectively. Thus the Q structure can be interpreted as due to the photoinduced *cis-trans* equilibrium in the side chains. In fact, the broadening of the features of $S(Q)$ may be due to the disordering effect due to the creation of a large number of *cis* conformers. Moreover, the fact that below RT $S(Q, \omega=0)$ decreases under the action of the light confirms that the photoinduced *cis-trans* equilibrium increases the mobility of the side chains (as confirmed by the photoinduced enhancement of the width of the QE signal, as already pointed out), leading to a general fluidification and a general disordering in the structure. This result is also confirmed by recent data on photoinduced effects on surface roughness of Langmuir-Schaefer multilayers of PA4 obtained by AFM microscopy and ellipsometry [15].

The temperature dependence of the photoinduced changes in the elastic signal is more difficult to interpret. First of all, the *cis-trans* thermally activated back relaxation is characterized by very long time constants (typically 2 h at RT, 5 min at 343 K [6]), therefore, it is always less important than the temperature-independent photoinduced back relaxation. Therefore, the change in the Q dependence of the elastic signal must be related to the fact that at about room temperature this material has a glass transition. It would be reasonable then that the increased general mobility would wipe out the Q structure. It is puzzling, however, that a structure of the opposite sign should appear at the higher temperature. We also recall the apparent independence of the QE broadening on temperature. Here, again the existence of a T_g in the middle of the temperature range, we explored might be significant. It is of interest, however, that the photoinduced broadening seems to disappear at the higher temperatures: this could be related to the fact that above T_g , the system has acquired general mobility and, hence, the fluidification effect of light becomes negligible. Clearly more precise data on the temperature dependence are needed, especially, at the higher temperatures.

We come now to the study of diffusional dynamics on the

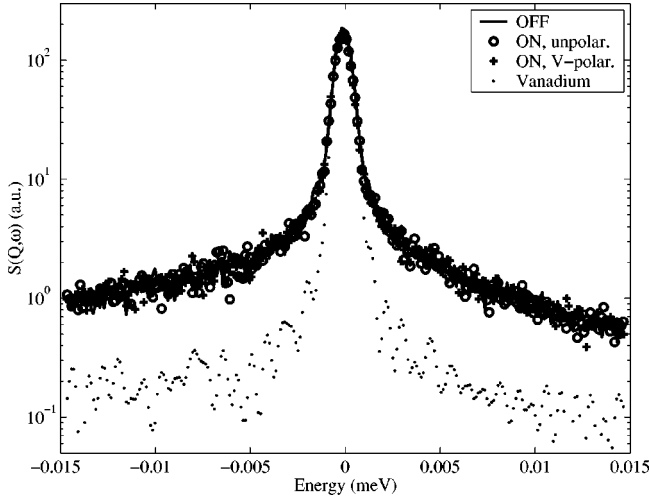


FIG. 7. Scattering law for PA4 measured on the backscattering IN16 at $T=300$ K, corresponding to an average exchanged momentum $Q=1.78 \text{ \AA}^{-1}$. Data are measured in dark, with UV unpolarized light on, and with UV V -polarized light (see text for details). The measured scattering laws are indistinguishable within the given S/N ratio. Also shown for comparison is the resolution function as determined from the vanadium calibration run.

slower time scale accessible by the backscattering IN16 spectrometer. In Fig. 7, we show the scattering law $S(Q, \omega)$ obtained on IN16, at $T=300$ K, and average exchanged momentum $Q=1.78 \text{ \AA}^{-1}$. On the time-energy scale of IN16 the fast motions studied with IN6 would appear as a flat background, if the line shape would be Lorentzian, as we had assumed in the simplified analysis as rotational diffusion. We can, however, not exclude that the observed quasielastic signal on IN16 is due to a very broad distribution of relaxation times. INS spectra were measured in the dark, with UV unpolarized light on, and with UV vertical (V) polarized light. As can be seen from the figure, the measured scattering laws measured with and without light are indistinguishable within our experimental signal to noise ratio. Also shown for comparison is the resolution function as determined from the vanadium calibration run, from which the presence of quasielastic broadening in our sample is evident.

The IN16 spectra were fit (see Fig. 8 for a typical fit) using the same model employed for the data of IN6, i.e., one elastic contribution (δ function) and one single QE contribution (Lorentzian shape), both convoluted with the experimental resolution function. From the Q dependence of the elastic intensity, we could extract the effective Debye-Waller mean square displacement $\langle u^2 \rangle$ as a function of the sample temperature. The results are summarized in Table I. We observe that at high temperature (340 K) the apparent mean square displacement estimated from the IN6 data at the same temperature is lower than that measured on IN16, this can be expected from the consideration of the time windows accessible with the resolution of the two instruments. Moreover, recalling that PA4 has $T_g=293$ K, the IN16 values of the mean square displacements are in complete agreement with the findings on typical polymeric systems by backscattering spectrometers, e.g., in atactic polystyrene ($T_g=375$ K)

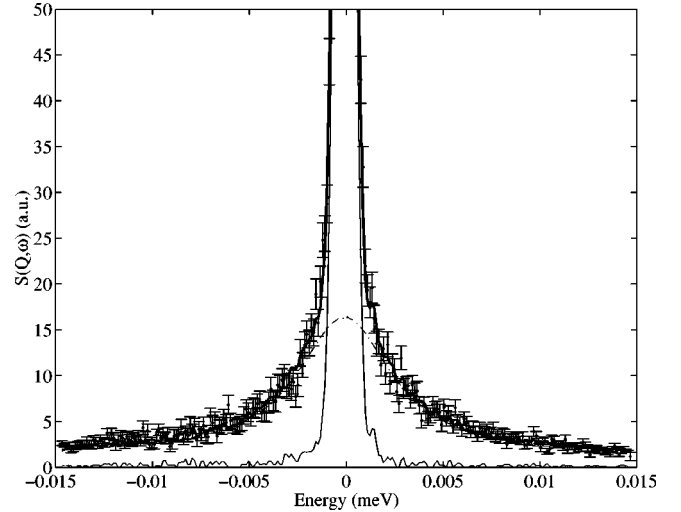


FIG. 8. A typical result of the fit (continuous line) of the quasielastic part of the backscattering INS spectrum of PA4 measured at $T=340$ K and $\langle Q \rangle=1.78 \text{ \AA}^{-1}$, using one Lorentzian (dash line) and one δ function, both convoluted with the experimental resolution function as determined by the vanadium standard (dash-dot line).

Frick *et al.* [22] found $\langle u^2 \rangle=0.3 \text{ \AA}^2$ at $T=T_g$, and $\langle u^2 \rangle=0.7 \text{ \AA}^2$ at 50 K above T_g .

The width of the QE component is found almost independent of the exchanged momentum Q , at least in the Q region above $Q=0.8 \text{ \AA}^{-1}$, with typical value $\text{FWHM}=2.0(5) \mu\text{eV}$ at $T=200$ K, and $\text{FWHM}=3.0(5) \mu\text{eV}$ at $T=304$ K, corresponding to correlation times ranging from 1.3 to 2 ns. The behavior of the FWHM with Q might indicate reorientational motion localized in space. Our data indicate that within experimental precision such motion is not affected by optical pumping, and, thus, it should not be connected with the azobenzene. Instead it could arise from the main chain conformational dynamics or from the part of the side chain located closer to the main chain.

In Fig. 9, we show the temperature dependence of the integrated quasielastic intensity measured for two average exchanged momenta: $\langle Q \rangle=0.71 \text{ \AA}^{-1}$ (open triangles) and $\langle Q \rangle=1.78 \text{ \AA}^{-1}$ (filled circles); we note that at both exchanged momenta the QE intensity starts to increase at about T_g ; this may be an indication of temperature activated increase in the population of mobile scatterers. However, it is worthwhile to note that well below T_g we have clearly a nonzero QE contribution. This correlates with the finding of a “fast” relaxation process in polystyrene well below T_g [22]. We also note the difference in the temperature increase

TABLE I. Temperature dependence of the Debye-Waller mean square displacement for PA4 ($T_g=293$ K) on IN16.

T/K	$\langle u^2 \rangle (\text{\AA}^2)$
200	0.12
304	0.35
340	0.75

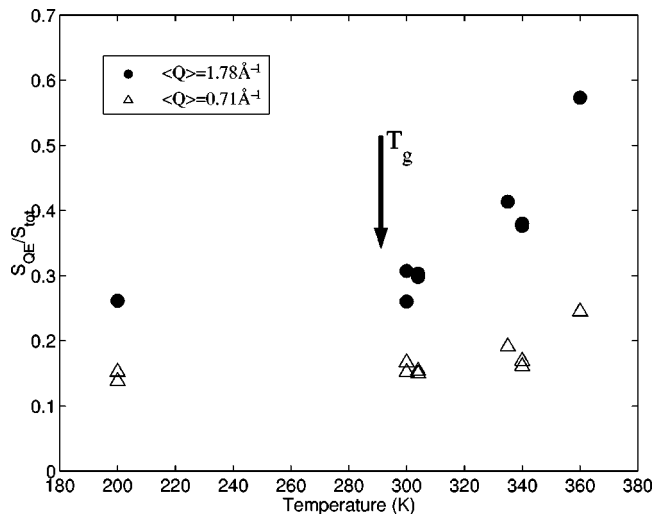


FIG. 9. Temperature dependence of the integrated quasielastic intensity at average momentum $\langle Q \rangle = 0.71 \text{ \AA}^{-1}$ (open triangles) and $\langle Q \rangle = 1.78 \text{ \AA}^{-1}$ (filled circles).

of the intensity at the two Q values shown. This indicates that the temperature activated mobility involves mainly reorientational fluctuations over short distances. On longer space scales, the material essentially retains its rigidity up to the highest temperature studied. Within this scenario, we can also find an interpretation for the disappearance of the optical effect of the FWHM seen with IN6 at high temperatures: in fact on the fast time scale of IN6 ($\sim 100 \mu\text{eV}$, e.g., $\sim 40 \text{ ps}$) the smaller size reorientational fluctuations are expected to give the dominant contribution, and these are the ones that are preferentially activated by the temperature increase.

The absence of optical effects on the IN16 spectra is extended to even slower time scales by the data we obtained with the spin-echo spectrometer IN11: here, too, no effect of optical pumping was observed on the time correlation function $S(Q, t)$ all the way to about $t = 10 \text{ ns}$. Thus, there is no appreciable coupling between the side chains and the main chain. This is different from what was observed on the fast time scale of IN6; there in parallel with the photoinduced changes in the QE scattering, we also observed changes in

the vibrational dynamics in the boson peak range, i.e., in the region of collective, acousticlike modes, which should be mainly related to the main chain motion. This is a good indication that the optically induced reorientational motion of the side chains influences the main chain low frequency vibrations, hence that there is coupling between the two chains on this time scale, whereas on longer space and time scales the two components are effectively uncoupled.

IV. CONCLUSIONS

In this work, we have presented an application of neutron scattering spectroscopy: namely, the study of optical effects on motional dynamics on the microscopic molecular scale. In particular, we studied the effects of *cis-trans* photoisomerization of the azobenzene moiety in a side chain liquid crystalline polymer. This material can be described by a two fluid ansatz: the side chain mesogenic and the main chain glassy phases. Taking advantage of the different time windows characteristic of the spectrometers we used, we have been able to demonstrate qualitatively the existence of a time structure in the coupling between these two fluids. In particular, we wish to emphasize the IN6 results, where the optical pumping of the *cis-trans* isomerization in the side chain influences the low frequency vibrational dynamics of the main chain. This implies an efficient coupling of the two fluids over the fast time and small distance scales. The two fluids become uncoupled as we approach the longer time and distance scales. However, given the difficulties of such pump-probe experiment that uses small amounts of material, our conclusions can only be qualitative and must be confirmed by more detailed studies: for instance, of the temperature dependence of the effects, and of selective deuteration of the side chains.

ACKNOWLEDGMENTS

We gratefully acknowledge Josè Dianoux (ILL) for many helpful discussions and for help with the time-of-flight experiment on IN6, G. Ehlers (ILL) for help with the spin echo IN11 experiment, and P. Camorani (University of Parma) for help with the experiments.

-
- [1] *Polymeric Liquid Crystals*, edited by A. Blumstein (Plenum Press, New York 1985); *Liquid-Crystal Polymers*, edited by N. A. Platè (Plenum Press, New York, 1993).
- [2] *Side Chain Liquid Crystal Polymers*, edited by C.B. Mc Ardle (Blackie and Sons, Glasgow, 1989); V.P. Shibaev, and N.A. Plate, *Comb-shaped Polymers and Liquid Crystals* (Plenum Press, New York, 1988); S. Hvilsted, F. Andruzzi, and P.S. Ramanujam, *Opt. Lett.* **17**, 1234 (1992); S. Hvilsted, F. Andruzzi, C. Kulima, H.W. Siesler, and P.S. Ramanujam, *Macromolecules* **28**, 2172 (1995).
- [3] M.P. Fontana, C. Paris, and M. Polli, *Mol. Cryst. Liq. Cryst.* **304**, 207 (1997).
- [4] L. Cristofolini, S. Arisi, and M.P. Fontana, *Synth. Met.* **124**, 151 (2002).
- [5] L. Andreatti, Ph.D. dissertation, University of Pisa, 1997; L. Andreatti, M.P. Fontana, F. Francia, M. Giordano, D. Leporini, and M. Rateo, *J. Non-Cryst. Solids* **172–174**, 943 (1994).
- [6] L. Cristofolini, P. Facci, P. Camorani, and M.P. Fontana, *J. Phys.: Condens. Matter* **11**, A359 (1999).
- [7] L. Cristofolini, S. Arisi, and M.P. Fontana, *Phys. Rev. Lett.* **85**, 4912 (2000).
- [8] A.S. Angeloni, D. Caretti, C. Carlini, E. Chiellini, G. Galli, A. Altomare, A. Solaro, and M. Laus, *Liq. Cryst.* **4**, 513 (1989).
- [9] A. Fontana, F. Rocca, M.P. Fontana, B. Rosi, and A.J. Dianoux, *Phys. Rev. B* **41**, 3778 (1990).

- [10] A complete survey of the work on the subject can be found, e.g., in the Proceedings of the Andalo Conferences on Disordered Systems. See, for instance, *Philos Mag. B* **79**, (1999) and *ibid.* **82** (2001).
- [11] S. Venugopalan and J. Rossabi, *J. Chem. Phys.* **85**, 5273 (1986).
- [12] M. Yasuniwa, S. Takim, and T. Takemura, *Mol. Cryst. Liq. Cryst.* **60**, 111 (1980).
- [13] P. Camorani, L. Cristofolini, and M.P. Fontana, *Mol. Cryst. Liq. Cryst.* (to be published).
- [14] L. Cristofolini, T. Berzina, M.P. Fontana, and O. Konovalov, *Mol. Cryst. Liq. Cryst.* (unpublished).
- [15] L. Cristofolini, M.P. Fontana, and O. Konovalov, *Philos. Mag. B* **82** (2002).
- [16] G. Gallone and M.P. Fontana, *Phys. Scr., T* **T57**, 168 (1995).
- [17] J.S. Higgins and H. Benoit, *Polymers and Neutron Scattering* (Oxford University Press, New York, 1994).
- [18] B. Frick and D. Richter, *Science* **267**, 1939 (1995).
- [19] A.S. Angeloni, D. Caretti, M. Laus, E. Chiellini, and G. Galli, *J. Polym. Sci., Part A: Polym. Chem.* **29**, 1865 (1991).
- [20] A.A. Craig, I. Winchester, P.C. Madden, P. Larcey, I.W. Hamley, and C.T. Imrie, *Polymer* **39**, 1197 (1998).
- [21] H. Gao and J.P. Harmon, *J. Appl. Polym. Sci.* **64**, 507 (1997).
- [22] B. Frick, U. Buchenau, and D. Richter, *Colloid Polym. Sci.* **273**, 413 (1995).